Published in final edited form as:
Biochim Biophys Acta. 2012 July ; 1823(7): 1163–1169. doi:10.1016/j.bbamcr.2012.04.015.

Insulin-like growth factor-1 (IGF-1) inhibits the basolateral Cl channels in the thick ascending limb of the rat kidney

Lijun Wang[1], **Wennan Li**[1], **Shumin Kong**[1], **Peng Wu**[1], **Chengbiao Zhang**[2], **Li Gu**[1], **Mingxiao Wang**[1], **WenHui Wang**[3], and **Ruimin Gu**[1]

[1]Department of Pharmacology, Harbin Medical University, Harbin, China 150086

[2]Institute of Anesthesiology, Xuzhou Medical College, Xuzhou, Jiangsu, China 221000

[3]Department of Pharmacology, New York Medical College, Valhalla, NY, 10595

Abstract

The aim of the present study is to test the hypothesis that insulin-like-growth factor-1 (IGF-1) plays a role in the regulation of basolateral Cl channels in the thick ascending limb (TAL). The patch-clamp experiments demonstrated that application of IGF-I or insulin inhibited the basolateral 10-pS Cl channels. However, the concentration of insulin required for the inhibition of the Cl channels by 50% ($K_{1/2}$) was ten times higher than those of IGF-1. The inhibitory effect of IGF-I on the 10-pS Cl channels was blocked by suppressing protein tyrosine kinase or by blocking phosphoinositide 3-kinase (PI3K). In contrast, inhibition of phospholipase C (PLC) failed to abolish the inhibitory effect of IGF-1 on the Cl channels in the TAL. Western blot analysis demonstrated that IGF-1 significantly increased the phosphorylation of phospholipid-dependent kinase (PDK) at serine residue 241 (Ser^{241}) and AKT at Ser^{473} in the isolated medullary TAL. Moreover, inhibition of PI3K with LY294002 abolished the effect of IGF-1 on the phosphorylation of PDK and AKT. The notion that the effect of IGF-1 on the 10-pS Cl channels was induced by stimulation of PDK-AKT-mTOR pathway was further suggested by the finding that rapamycin completely abolished the effect of IGF-1 on the 10-pS Cl channels in the TAL. We conclude that IGF-1 inhibits the basolateral Cl channels by activating PI3K-AKT-mTOR pathways. The inhibitory effect of IGF-1 on the Cl channels may play a role in ameliorating the ischemia-induced renal injury through IGF-1 administration.

Keywords

phosphoinositide 3-kinase; PKD; AKT; mTOR; Cl transport

1. Introduction

IGF-1, IGF-1 receptor (IGF-1R) and IGF-1 binding proteins are three important components of IGF-1 system [1,2]. IGF-1 mRNA was detected in the TAL of Henle's loop in the outer medulla while IGF-1R mRNA was expressed throughout the kidney including medullary

Corresponding address: Dr. WenHui Wang, Department of Pharmacology, New York Medical College, 15 Dana Road, Valhalla, NY 10595, (tel) 914 594 4139, (Fax) 914 347 4956, wenhui_wang@nymc.edu or Dr. Ruimin Gu, Department of Pharmacology, Harbin Medical University, Harbin, China 150086, ruimingu2916@yahoo.com.cn.

TAL [3,4]. IGF-1 binding protein mRNA was located in both TAL and distal convoluted tubule [4]. IGF-1 has been shown to stimulate epithelial Na channels in the collecting duct cells [5]. We have previously shown that IGF-1 had a biphasic effect on the apical 70 pS K channel which plays a key role in the apical K recycling in the TAL: IGF-1 at low concentrations stimulated while at high concentrations inhibited the apical 70-pS K channels [6]. Since the K recycling is essential for maintaining the activity of the apical Na/K/Cl cotransporter (NKCC2) in the TAL [7–9], it is possible that IGF-1-induced inhibition of apical K channels may lead to decreasing NKCC2 activity. It was well documented that the activity of NKCC2 was also affected by the alteration in intracellular Cl concentrations [10]. Thus, we speculate that IGF-1 at high concentrations may inhibit not only the apical K channels but also the basolateral Cl channels in the TAL. This speculation is also supported by the fact that IGF-1R is highly expressed in the basolateral membrane of renal tubules [11]. Therefore, the aim of the present study is to explore the role of IGF-1 in regulating the basolateral 10-pS Cl channels which are the main type of Cl channels in the TAL [12,13].

2. Material and Methods

2.1. Preparation of medullary TAL

Sprague-Dawley rats of either sex (70–90 g) were obtained from the Animal Center of the Second Affiliated Hospital of Harbin Medical University (Harbin, China). The animals were fed with a normal rat chow. After rats were sacrificed with cervical dislocation, both kidneys were removed immediately and they were cut into several 1-mm thick slices along coronal plane with a razor blade. The kidney slices were then incubated at 37°C in a solution containing collagenase type IA (1 mg/ml) (Sigma, St. Louis, MO) for 45~60 minutes. After the collagenase treatment, the kidney slices were rinsed three times with a solution containing (in mM): 140 NaCl, 5 KCl, 1.8 $MgCl_2$, 1.8 $CaCl_2$, and 10 HEPES (pH=7.4) at 4°C. The tubules were dissected with fine watch-maker forceps under the dissection microscope. The isolated medullary TALs were adhered to a cover glass (5×5 mm) coated with Poly-D-lysine (Sigma, St Louis, MO). The cover glass was transferred into a chamber (1 ml) mounted on an inverted Nikon microscope and the TALs were superfused with the HEPES-buffered bath solution containing (in mM) 140 NaCl, 5 KCl, 1.8 $CaCl_2$, 1.8 $MgCl_2$, 5 mM glucose and 10 HEPES (pH=7.4). The animal protocol was approved by the animal care and use committee of Harbin Medical University.

2.2. Patch-clamp technique

The patch pipettes were pulled with Narishige PP-830 electrode-puller, polished by WPI MF-200 electrode-polisher, and filled with the pipette solution containing (in mM): 140 NaCl, 1.8 $MgCl_2$, and 10 HEPES (pH=7.4). We used an Axon 200B patch-clamp amplifier to record channel currents which were low-pass filtered at 0.2–0.5 KHz and digitized by an Axon interface (Digidata 1320). Data were analyzed using pClamp software system 9.2 (Axon Instruments, Burlingame, CA). Channel activities were defined as NP_o, a product of channel open probability (P_o) and channel number (N). The NP_o was calculated from data samples of 60s duration in the steady state using following equation:

$$NP_o = \sum (1t_1 + 2t_2 + \ldots it_i)$$

in which t_i is the fractional open time spent at each of the observed current levels. We used an all-point histogram to calculate the channel activity. The slope conductance of the channel was determined by measurement of the current amplitude at several holding potentials. All experiments were performed in cell-attached patches. Since the onset time of

IGF-1 was typically within 5–6 min, we selected a 60-min-long recording at the steady state of channel activity at least 5–6 min after adding IGF-1.

2.3. Western blot

The protein sample (100 g) obtained from isolated medullary TAL was separated by electrophoresis using 8% SDS-PAGE and transferred to nitrocellulose membranes. Membranes were blocked with 5% nonfat dry milk in 0.1% Tween-Tris-buffered saline (TBS-T) and washed with 0.1% TBS-T. The membranes were incubated overnight at 4 °C with the corresponding primary antibody. After four times 10-min wash with TBS-T, the membrane was incubated with the secondary antibody for additional one hr. ECL plus (Thermo Fisher Scientific Inc.) was used to detect the protein bands.

2.4 Chemicals and experimental solution

Antiphospho-Akt-Ser473 and AKT antibodies were obtained from Cell Signaling Technology (Billerica, MA) while antiphospho-PDK-Ser241 and PDK antibodies were purchased from Santa Cruz Biotechnology (Santa Cruz, CA). IGF-1, insulin and other chemicals were purchased from Sigma (St Louis, MO). IGF-I and insulin were dissolved in deionized water containing 0.1% acetic acid and other chemicals (genestein, herbimycin A, Ly294002, wortmannin, U73122, and rapamycin) were dissolved in DMSO. The final concentration of DMSO in the bath was less than 0.1% and DMSO at 0.1% concentration did not affect the Cl channel activity. During the experiments we added genestein, herbimycin A, Ly294002, wortmannin, U73122, and rapamycin to the bath and the tubules were incubated in such bath solution for at least 5–6 min before applying IGF-1 subsequently.

2.5. Statistics

Data are shown as means ± SEM We used paired Student's *t*-tests to determine the significance of the difference between the control and experimental periods. Statistical significance was taken as $P<0.05$.

3. RESULTS

We confirmed the observations reported by our group and other investigators that the 10-pS Cl channel was the main type of Cl channels in the basolateral membrane of the medullary TAL [12,13]. Therefore, the present study is focused on examining the effect of IGF-1 on the basolateral 10-pS Cl channels. Figure 1A is a recording showing Cl channel activity under control conditions and after addition of IGF-1 (200 nM). The average number of the 10-pS Cl channel in each patch was two and the mean channel activity (NP_o) was 1.03±0.07 (n=10). Application of IGF-I inhibited the basolateral 10-pS Cl channel in a cell-attached patch. within 5–6 min. Fig. 1B is a dose response curve of IGF-1 effect showing that IGF-1 at concentrations higher than 50 nM significantly inhibited the 10-pS Cl channel. Moreover, application of 300 nMIGF-1 induced a maximal inhibition of 10-pS Cl channel and decreased channel activity (defined by NP_o) from 1.03±0.07 to 0.05±0.03 (n=10, $p<0.01$). We estimated that the concentration of IGF-1 required for inhibition of Cl channels by 50% ($K_{1/2}$) was approximately 120 nM. Since IGF-1R could be activated also by insulin, we examined whether insulin could mimic the effect of IGF-1 and inhibit Cl channels in the TAL. Figure 2A is a channel recording showing the effect of insulin (1 μM) on the 10-pS Cl channels. It is apparent that insulin was able to inhibit the 10-pS Cl channel within 10 min. However, the inhibitory effect of insulin on the Cl channels was less potent than that of IGF-1. Fig. 2B is a dose response curve of insulin-induced inhibition of the 10-pS Cl channel in the TAL and the estimated $K_{1/2}$ value was approximately 1200 nM, a value was ten times higher than that of IGF-1. Thus, the effect of IGF-1 on the Cl channels was

specifically related to IGF-1R. Since 200 nM IGF-1 caused a sub maximal inhibition of the Cl channels, we used 200 nM IGF-1 through out the study.

Activation of IGF-1R is expected to stimulate tyrosine kinase activity through beta-subunit of IGF-1R [14]. Therefore, we examined whether inhibition of tyrosine kinase activity could abolish the effect of IGF-1 on the 10-pS Cl channels. Fig. 3 is a channel recording demonstrating the effect of 200 nM IGF-1 on the Cl channels in the TAL treated with Herbimycin A, an inhibitor of protein tyrosine kinase [15]. Treatment of the TAL with Herbimycin A (1 μM) did not significantly affect the 10-pS Cl channel activity within 10 min (Control NPo, 0.98±0.1; Herbimycin A, 0.97±0.08) (N=6). However, inhibition of tyrosine kinase abolished the effect of IGF-1 on the Cl channels (NPo, 0.99±0.1, n=6). In contrast, IGF-1 decreased Cl channel activity to 0.24±0.05 (n=5) in the absence of Herbimycin A (Fig.4B). Similar results were observed in the TAL treated with genistein. Fig. 4A is a channel recording demonstrating that 200 nM IGF-1 failed to inhibit the 10-pS Cl channels in the presence of genistein (10 μM). Data summarized from 8 experiments were shown in a bar graph (Fig.4B) (control NPo, 0.98±0.1; genistein, NPo, 1.01±0.1; genistein+IGF-1, 1.03±0.1).

After demonstrating the role of tyrosine kinase activity in mediating the effect of IGF-I on the basolateral 10-pS Cl channels, we examined whether PI3K, a down stream signaling molecule of IGF-1 pathway, was involved in modulating the effect of IGF-1 on the 10-pS Cl channels. Figure 5A is a representative channel recording in a cell-attached patch demonstrating that treatment of the mTAL with LY294002 (10 μM), a specific inhibitor of PI3K [16], abolished the effect of 200 nM IGF-I on 10-pS Cl channels. Results summarized in Fig. 5B show that 200 nM IGF-I failed to inhibit the 10-pS Cl channel (control NPo, 1.02±0.1; LY294002, 1.08±0.1; LY294002+IGF-1, 1.06±0.1) (N=7). The same results were observed with wortmannin, another specific inhibitor of PI3K [17]. Fig. 5C is a channel recording showing that the effect of IGF-1 on the Cl channels was absent in the mTAL treated with 100 nM wortmannin.. Data summarized in Fig. 5B demonstrate that application of 200 nM IGF-1 had no significant effect on the Cl channel activity in the TAL treated with wortmannin (Wortmannin NPo, 1.15±0.08; Wortmannin+IGF-1, 1.08±0.08) (n=6). The results suggest that PI3K is involved in mediating the effect of IGF-1 on the Cl channels in the TAL.

Activation of PI3K has been shown to stimulate phospholipase C (PLC) or AKT [18,19]. Therefore, we first examined the role of PLC in mediating the effect of IGF-1 on the 10-pS Cl channels in the TAL. Fig. 6A is a channel recording demonstrating that the effect of 200 nM IGF-I on the 10-pS Cl channel in the presence of U73122 (5 μM). Inhibition of PLC did not significantly affect the basal activity of the 10-pS Cl channels (NP_o, 1.31±0.13), a value not significantly different from the control (NP_o=1.19±0.12) (Fig. 6B). However, addition of 200 nM IGF-I decreased NP_o to 0.27±0.1 in the presence of U73122, suggesting that the effect of IGF-I was not mediated by PLC dependent pathway.

Stimulation of PI3K has been demonstrated to activate AKT either by PDK or by phosphatidylinositol (3,4,5)-triphosphate (PIP3) [19]. To test whether IGF-1 activates PDK in the TAL, we examined the effect of IGF-1 on PDK phosphorylation using antibody reacting to phosphorylated PDK at serine residue 241 (P-PDK^{S241}), an indication of PDK activation [20], in the isolated medullary TAL treated with 200 nM IGF-1 for 5, 15, 30 min, respectively. Fig. 7A is a Western blot demonstrating the time course of IGF-1 on PDK phosphorylation. It is apparent that incubation of the medullary TAL with 200 nM IGF-1 for 5 min increased P-PDK^{S241} by 190±20% (N=3 rats). Results were also consistent with the patch-clamp experiments in which IGF-1 inhibited 10-pS Cl channels within 5–6 min (Fig. 1). We next examined the dose response curve of the effect of IGF-1 on PDK

phosphorylation by treating the medullary TAL with 100, 200 and 300 nM IGF-1 for 5 min. As shown in Fig. 7B, 200 nM IGF-1 caused a sub-maximal stimulation of P-PDK^{S241} by 195±20%. To determine whether IGF-1-induced stimulation of P-PDK^{S241} was PI3K-dependent, we examined the effect of IGF-1 on the phosphorylated PDK in the presence of LY294002. From inspection of Fig. 7C, it is apparent that inhibition of PI3K completely abolished the effect of IGF-1 (200 nM) on P-PDK^{S241} (90±10% of the control value) (N=3 rats).

Not only stimulating PDK phosphorylation, IGF-1 (200 nM) also increased phosphorylation of AKT at Ser^{473} (P-AKT^{S473}), an indication of AKT activation [20]. Fig. 8A is a Western blot from 3 similar experiments (3 rats) in which the effect of 200 nM IGF-1 on P-AKT^{S473} was examined with specific antibody reacting with Ser^{473} of AKT in the isolated medullary TAL treated with or without 10 μM LY294002. IGF-1 increased the AKT phosphorylation by 180±20%, an effect was absent in the medullary TAL treated with LY294002 (Fig. 8B). Therefore, the results strongly suggest that IGF-1-induced inhibition of the basolateral 10-pS Cl channel is mediated by PDK-AKT pathways.

AKT has been shown to activate mTOR directly through the phosphorylation or indirectly through tuberous-sclerosis-complex-dependent mechanism [19]. To examine the role of mTOR, we used rapamycin, which specifically binds to and inhibits the mTOR [21,22]. Rapamycin has been widely used as a tool for exploring the role of mTOR in mediating the function of IGF-1 in a variety of tissue [23–25]. We tested whether inhibition of mTOR was able to block the effect of IGF-1 on the 10-pS Cl channels. Figure 9A is a representative channel recording showing that IGF-I did not inhibit the 10-pS Cl channel in the presence of rapamycin (100 nM). Fig. 9B summarizes the results from six experiments showing that rapamycin abolished the inhibition of the Cl channels by IGF-1 (1.1±0.1) while it had no significant effect on the channel activity (NP_o, 1.14±0.1) (N=5). Therefore, the results suggest the role of mTOR in mediating the inhibitory effect of IGF-I on the 10-pS Cl channel in the TAL.

4. DISCUSSION

The main finding of the present study is that IGF-1 inhibits the basolateral 10-pS Cl channels by PI3K-dependent pathway. Although insulin could also inhibit the 10-pS Cl channel, the $K_{1/2}$ value was one order of magnitude higher than those of IGF-1, suggesting that the effect of insulin may be mediated by stimulating IGF-1R. Thus, IGF-1R may play a role in regulating basolateral Cl conductance. The Cl channel plays an important role in maintaining NaCl transport in the TAL [26]. The transepithelial Cl transport in the TAL is achieved by a two-step process: Cl enters the cell through the apical NKCC2 and leaves the cells through the basolateral Cl channels or KCl cotransporter.[27]. Molecular cloning has identified two types of Cl channels, ClC-K1 and ClC-K2 in the Henle's loop [28,29]. Moreover, immunostaining demonstrates that ClC-K1 is mainly expressed in the thin ascending limb of Henle's loop [30] while ClC-K2 is predominantly expressed in the basolateral membrane of the TAL in the rat kidney [31], suggesting that ClC-K2 is responsible for the basolateral Cl conductance. This view is strongly indicated by the finding that defective gene product encoding either ClC-K2 or barttin caused type IV Barter's syndrome [32]. Patch-clamp studies have demonstrated that two types of Cl channels, an 8–9 pS and a 20–40 pS, are expressed in the basolateral membrane of the TAL and that the 8–9 pS Cl channel is a main type of Cl channels expressed in the basolateral membrane [13]. Thus, it is most likely that 10-pS Cl channel is the gene product of ClC-K2. Therefore, inhibition of the basolateral Cl channels by IGF-1 is expected to increase the intracellular Cl concentration thereby decreasing the activity of NKCC2 in the TAL by inhibition of Ste20-related Prolin/Alanine-Rich kinase [10].

It is well documented that activation of IGF-1R stimulates the tyrosine phosphorylation of IGF-1R's β-subunit thereby initiating IGF-mediated signaling pathway [14]. The observation that inhibition of tyrosine kinase activity abolished the inhibitory effect of IGF-1 on the basolateral 10-pS Cl channels strongly suggests the role of tyrosine kinase in mediating the effect of IGF-1 on the Cl channels. We proposed that the effect of IGF-1 on the basolateral 10-pS Cl channels is mediated by PI3K-AKT-mTOR pathways. First, suppresing PI3K or mTOR completely abolished the inhibition of the Cl channels by IGF-1. Second, application of IGF-1 increased PDK phosphorylation at Ser^{241} and AKT at Ser^{473}. Third, inhibition of PI3K abolished the effect of IGF-1 on PDK and AKT phosphorylations in the TAL.

IGF-1 has been shown to increase renal blood flow and glomerular filtration rate in the kidney [33,34] and to facilitate the tubular remodeling and repair after ischemic insult [35]. We have previously demonstrated that IGF-1 regulates the apical 70-pS K channels in the TAL by a biphasic manner: IGF-1 at low concentrations stimulates while at high concentrations inhibits the 70-pS K channels [6]. In the present study, IGF-1 at physiological relevant concentrations (less than 50 nM) had no effect on the Cl channels while at high concentrations IGF-1 inhibited the Cl channels in the TAL. Insulin and IGF-1 have been shown to increase transepithelial Na transport in the aldosterone-sensitive distal nephron by stimulation of amiloride-sensitive ENaC [5,36,37]. Moreover, acute IGF-1 infusion at 50 nM has been shown to induce antidiuretic and antinatriuretic effects by increasing phosphorylation of NKCC2 [38] In contrast, the present study demonstrated that IGF-1 at concentrations larger than 50 nM inhibited the basolateral Cl channels. The discrepancy may be induced not only by different nephron segments (collecting duct vs TAL) but also different concentrations of insulin or IGF-1 used in experiments. It is possible IGF-1/insulin at physiological concentrations may stimulate renal Na absorption but it has no effect on the basolateral Cl channels. However, IGF-1 at high concentrations might decrease Na absorption through inhibition of Cl transport in the TAL. Relevant to our hypothesis is the report that natriuretic response induced by loop diuretics was lower in rats with high basal level of IGF-1 and other growth hormones (GC rats) than those of the control rats [36]. IGF-1-induced increase in ENaC activity in the aldosterone-sensitive distal nephron may be partially responsible for the diminished effect of furosemide on renal Na excretion [36]. However, it is also possible that IGF-1 may decrease Na transport in the mTAL by directly inhibiting NKCC2 or through inhibiting basolateral Cl channels thereby indirectly decreasing NKCC2 activity in the TAL. Thus, furosemide-induced natriuretic effect in the TAL is attenuated in rats with high IGF-1 level. The notion that IGF-1 may differently regulate ENaC in the collecting duct and basolateral Cl channels in the TAL is also suggested by the report that renal Na excretion in GC rats was not significantly different from those of the control rats with a normal basal level of IGF-1 [36].

It has been shown that normal plasma concentrations of IGF-1 in rats or mice are between 340 and 400 ng/ml or 45 and 50 nM under physiological conditions [39,40] and the serum levels of IGF-I in human is between 25 to 40 nM. [41]. Thus, the concentrations of IGF-1 used in the present study were not in the physiological relevant ranges. However, it has been shown that the bioavailability of IGF-1 might increase significantly by lowering IGF-1 binding protein after acute renal failure [42]. Moreover, infusion of IGF-1 has been shown to ameliorate transient ischemia-induced acute renal failure in rats [43] and to facilitate the renal recovery after ischemia-induced acute renal failure [44]. IGF-1 has been used in the clinical practice to treat acute or chronic renal failure [45]. Fig 10 is a cell scheme illustrating a possible mechanism by which IGF-1 inhibits the basolateral 10-pS Cl channels in the medullary TAL. Since the 10-pS Cl channel is the main type of the Cl channels in the basolateral membrane of the TAL, inhibition of the basolateral Cl channels by IGF-1 is expected to diminish the transepithelial Cl absorption thereby decreasing oxygen

consumption in the medullary TAL. Thus, IGF-1-induced inhibition of the basolateral Cl channels could be a possible factor which protects the TAL after ischemia. We conclude that IGF-1 inhibits the basolateral 10-pS Cl channels in the TAL by PI3K-AKT-mTOR pathways. The significance of the present finding may illustrate a new mechanism by which IGF-1 protects kidney from ischemia-induced injury through suppressing transepithelial Cl transport in the medullary TAL.

Acknowledgments

The work is supported by Chinese National Natural Science Foundation #31171110 (RMG) and #31171109 (CBZ), PIF#YJSCX2011-331HLJ (LJW) and NIH grant HL34100 (WHW).

References

1. Hammerman MR. The growth hormone-insulin-like growth factor axis in kidney. Am J Physiol. 1989; 257(Renal 26):503–514.
2. Jones JI, Clemmons DR. Insulin-like growth factor and their binding proteins:Biological action. Endocrine Rev. 1995; 15:3–34. [PubMed: 7758431]
3. Rabkin R, Brody M, Lu LH, Chan C, Shaheen AM, Gillett N. Expression of the gene encoding the rat renal insulin-like growth factor-1 system. J Am Soc Nephrol. 1995; 6:1511–1518. [PubMed: 8589331]
4. Chin E, Zhou J, Bondy CA. Renal growth hormone receptor gene expression: relationship to renal insulin-like growth factor system. Endocrinology. 1992; 131:3061–3066. [PubMed: 1446640]
5. Gonzalez-Rodriguez E, Gaeggeler HP, Rossier BC. IGF-1 vs insulin: Respective roles in modulating sodium transport via the PI-3 kinase//Sgk1 pathway in a cortical collecting duct cell line. Kidney Int. 2006; 71:116–125. [PubMed: 17164836]
6. Wei Y, Chen YJ, Li D, Gu R, Wang WH. Dual effect of insulin-like growth factor on the apical 70-pS K channel in the thick ascending limb of rat kidney. American Journal of Physiology - Cell Physiology. 2004; 286:C1258–C1263. [PubMed: 15151916]
7. Simon DB, Lifton RP. The molecular basis of inherited hypokalemic alkalosis: Bartter's and Gitelman's syndromes. Am J Physiol (Renal Fluid Electrolyte Physiol). 1996; 271:F961–F966.
8. Hebert SC. Bartter syndrome. Curr Opin Nephrol Hypertens. 2003; 12:527–532. [PubMed: 12920401]
9. Simon DB, Karet FE, Rodriguez-Soriano J, Hamdan JH, DiPietro A, Trachtman H, Sanjad SA, Lifton RP. Genetic heterogeneity of Bartter's syndrome revealed by mutations in the K^+ channel, ROMK. Nature Genetics. 1996; 14:152–156. [PubMed: 8841184]
10. Ponce-Coria J, San Cristobal P, Kahle KT, Vazquez N, Pacheco-Alvarez D, los Heros P, Juarez P, Munoz E, Michel G, Bobadilla NA, Gimenez I, Lifton RP, Hebert SC, Gamba G. Regulation of NKCC2 by a chloride-sensing mechanism involving the WNK3 and SPAK kinases. Proceedings of the National Academy of Sciences. 2008; 105:8458–8463.
11. Hise MK, Lahn JS, Shao ZM, Mantzouris NM, Fontana JA. Insulin-like growth factor-I receptor and binding proteins in rat kidney after nephron loss. J Am Soc Nephrol. 1993; 4:62–68. [PubMed: 7691204]
12. Gu RM, Yang L, Zhang Y, Wang L, Kong S, Zhang C, Zhai Y, Wang M, Wu P, Liu L, Gu F, Zhang J, Wang WH. CYP-omega-hydroxylation-dependent metabolites of arachidonic acid inhibit the basolateral 10[thinsp]pS chloride channel in the rat thick ascending limb. Kidney Int. 2009; 76:849–856. [PubMed: 19641481]
13. Guinamard R, Chraibi A, Teulon J. A small-conductance Cl- channel in the mouse thick ascending limb that is activated by ATP and protein kinase A. J Physiol. 1995; 485:97–112. [PubMed: 7658386]
14. Siddle K. Signalling by insulin and IGF receptors: supporting acts and new players. Journal of Molecular Endocrinology. 2011; 47:R1–R10. [PubMed: 21498522]

15. Satoh T, Uehara Y, Kaziro Y. Inhibition of Interleukin 3 and granulocytes-macrophage colony-stimulating factor stimulated increase of active Ras-GTP by herbimycin A, a specific inhibitor of tyrosine kinases. J Biol Chem. 1992; 267:2537–2541. [PubMed: 1733950]

16. Vlahos CJ, Matter WF, Hui KY, Brown RF. A specific inhibitor of phosphatidylinositol 3-kinase, 2-(4-morpholinyl)-8-phenyl-4H-1-benzopyran-4-one (LY294002). J Biol Chem. 1994; 269:5241–5248. [PubMed: 8106507]

17. Xie LH, Takano M, Kakei M, Okamura M, Noma A. Wortmannin, an inhibitor of phosphatidylinositol kinases, blocks the MgATP-dependent recovery of Kir6.2/SUR2A channels. J Physiol. 1999; 514(Pt 3):655–665. [PubMed: 9882737]

18. Reynolds LF, Smyth LA, Norton T, Freshney N, Downward J, Kioussis D, Tybulewicz VLJ. Vav1 Transduces T Cell Receptor Signals to the Activation of Phospholipase C-gamma1 via Phosphoinositide 3-Kinase-dependent and -independent Pathways. The Journal of Experimental Medicine. 2002; 195:1103–1114. [PubMed: 11994416]

19. Hollander MC, Blumenthal GM, Dennis PA. PTEN loss in the continuum of common cancers, rare syndromes and mouse models. Nat Rev Cancer. 2011; 11:289–301. [PubMed: 21430697]

20. Gines S, Ivanova E, Seong IS, Saura CA, MacDonald ME. Enhanced Akt Signaling Is an Early Pro-survival Response That Reflects N-Methyl-D-aspartate Receptor Activation in Huntington's Disease Knock-in Striatal Cells. J Biol Chem. 2003; 278:50514–50522. [PubMed: 14522959]

21. Ballou LM, Selinger ES, Choi JY, Drueckhammer DG, Lin RZ. Inhibition of Mammalian Target of Rapamycin Signaling by 2-(Morpholin-1-yl)pyrimido[2,1-+¦]isoquinolin-4-one. J Biol Chem. 2007; 282:24463–24470. [PubMed: 17562705]

22. Bolster DR, Crozier SJ, Kimball SR, Jefferson LS. AMP-activated Protein Kinase Suppresses Protein Synthesis in Rat Skeletal Muscle through Down-regulated Mammalian Target of Rapamycin (mTOR) Signaling. J Biol Chem. 2002; 277:23977–23980. [PubMed: 11997383]

23. Liu L, Luo Y, Chen L, Shen T, Xu B, Chen W, Zhou H, Han X, Huang S. Rapamycin Inhibits Cytoskeleton Reorganization and Cell Motility by Suppressing RhoA Expression and Activity. J Biol Chem. 2010; 285:38362–38373. [PubMed: 20937815]

24. Kwon J, Stephan S, Mukhopadhyay A, Muders MH, Dutta SK, Lau JS, Mukhopadhyay D. Insulin Receptor Substrate-2 Mediated Insulin-like Growth Factor-I Receptor Overexpression in Pancreatic Adenocarcinoma through Protein Kinase C+¦. Cancer Res. 2009; 69:1350–1357. [PubMed: 19190347]

25. Harwood FC, Shu L, Houghton PJ. mTORC1 Signaling Can Regulate Growth Factor Activation of p44/42 Mitogen-activated Protein Kinases through Protein Phosphatase 2A. J Biol Chem. 2008; 283:2575–2585. [PubMed: 18056704]

26. Reeves WB, Winters CJ, Andreoli TE. Chloride channels in the loop of Henle. Annu Rev Physiol. 2001; 63:631–645. [PubMed: 11181970]

27. Greger R. Ion transport mechanisms in thick ascending limb of Henle's loop of mammalian nephron. Physiol Rev. 1985; 65:760–797. [PubMed: 2409564]

28. Kieferle S, Fong P, Bens M, Vandewalle A, Jentsch TJ. Two highly homologous members of the ClC chloride channel family in both rat and human kidney. Proc Natl Acad Sci, USA. 1994; 91:6943–6947. [PubMed: 8041726]

29. Adachi S, Uchida S, Ito H, Hata M, Hiroe M, Marumo F, Sasaki S. Two isoforms of a chloride channel predominantly expressed in thick ascending limb of Henle's loop and collecting ducts of rat kidney. J Biol Chem. 1994; 269:17677–17683. [PubMed: 8021279]

30. Uchida S, Sasaki S, Nitta K, Uchida K, Horita S, Nihei H, Marumo F. Localization and functional characterization of rat kidney-specific chloride channel, ClC-K1. J Clin Invest. 1995; 95:104–113. [PubMed: 7814604]

31. Winters CJ, Zimniak L, Reeves WB, Andreoli TE. Cl- channels in basolateral renal medullary membranes XII. Anti-rbClC-Ka antibody blocks MTAL Cl- channels. AJP - Renal Physiology. 1997; 273:F1030–F1038.

32. Simon DB, Bindra RS, Mansfield TA, Nelson-Williams C, Mendonça E, Stone R, Schurman S, Nayir A, Alpay H, Bakkaloglu A, Rodriguez-Soriano J, Morales JM, Sanjad SA, Taylor CM, Pilz D, Brem A, Trachtman H, Griswold W, Richard GA, John E, Lifton RP. Mutations in the chloride

channel gene, *CLCNKB*, cause Bartter's syndrome type III. Nature Genetics. 1997; 17:171–178. [PubMed: 9326936]

33. Hirschberg R, Kopple JD. Evidence that IGF-1 increases renal plasma flow and glomerular filtration rate in fasted rats. J Clin Invest. 1989; 83:326–330. [PubMed: 2910916]
34. Guler HP, Schmid C, Zapf J, Froesch ER. Effects of rIGF-I on insulin secretion and renal function in narmal human subjects. Proc Natl Acad Sci. 1989; 86:2868–2872. [PubMed: 2649897]
35. Gobe G, Willgoss D, Hogg N, Schoch E, Endre Z. Cell survival or death in renal tubular epithelium after ischemia-reperfusion injury. Kidney Int. 1999; 56:1299–1304. [PubMed: 10504480]
36. Kamenicky P, Viengchareun S, Blanchard A, Meduri G, Zizzari P, Imbert-Teboul M, Doucet A, Chanson P, Lombes M. Epithelial Sodium Channel Is a Key Mediator of Growth Hormone-Induced Sodium Retention in Acromegaly. Endocrinology. 2008; 149:3294–3305. [PubMed: 18388193]
37. Staruschenko A, Pochynyuk O, Vandewalle A, Bugaj V, Stockand JD. Acute Regulation of the Epithelial Na+ Channel by Phosphatidylinositide 3-OH Kinase Signaling in Native Collecting Duct Principal Cells. J Am Soc Nephrol. 2007; 18:1652–1661. [PubMed: 17442787]
38. Dimke H, Flyvbjerg A, Bourgeois S, Thomsen K, Frokiaer J, Houillier P, Nielsen S, Frische S. Acute growth hormone administration induces antidiuretic and antinatriuretic effects and increases phosphorylation of NKCC2. American Journal of Physiology - Renal Physiology. 2007; 292:F723–F735. [PubMed: 17062845]
39. Takeda R, Nishimatsu H, Suzuki E, Satonaka H, Nagata D, Oba S, Sata M, Takahashi M, Yamamoto Y, Terauchi Y, Kadowaki T, Kangawa K, Kitamura T, Nagai R, Hirata Y. Ghrelin Improves Renal Function in Mice with Ischemic Acute Renal Failure. J Am Soc Nephrol. 2006; 17:113–121. [PubMed: 16306169]
40. Evan EP, Henry DP, Connors BA, Summerlin P, Lee WH. Analysis of insulin-like growth factor (IGF)-1, and II, type II IGF receptor and IGF-binding protein-1 mRNA and peptide levels in normal and nephrectomized rat kidney. Kidney Int. 1995; 48:1517–1529. [PubMed: 8544409]
41. Wang SN, Lapage J, Hirschberg R. Glomerular ultrafiltration and apical tubular action of IGF-I, TGF-[bgr], and HGF in nephrotic syndrome. Kidney Int. 1999; 56:1247–1251. [PubMed: 10504466]
42. Tsao T, Wang J, Fervenza FC, Vu TH, Jin IH, Hoffman AR, Rabkin R. Renal growth hormone[mdash]Insulin-like growth factor-I system in acute renal failure. Kidney Int. 1995; 47:1658–1668. [PubMed: 7543960]
43. Noguchi S, Kashihara Y, Ikegami Y, Morimoto K, Miyamoto M, Nakao K. Insulin-like growth factor-I ameliorates transient ischemia-induced acute renal failure in rats. Journal of Pharmacology And Experimental Therapeutics. 1993; 267:919–926. [PubMed: 8246168]
44. Miller SB, Martin DR, Kissane J, Hammerman MR. Rat models for clinical use of insulin-like growth factor I in acute renal failure. American Journal of Physiology - Renal Physiology. 1994; 266:F949–F956.
45. Hammerman MR, Miller SB. Therapeutic use of growth factors in renal failure. J Am Soc Nephrol. 1994; 5:1–11. [PubMed: 7948775]

Highlights

- The patch-clamp experiments were performed in the thick ascending limb(TAL).
- Application of 200 nM IGF-1 inhibited the basolateral Cl channels in the TAL.
- The basolateral Cl channel is a rate limiting step for Cl exit in the TAL cells.
- Rising intracellular Cl level leads to inhibition trans-cellular Cl transport.
- IGF-1 at high concentration may inhibit epithelial transport in the TAL.

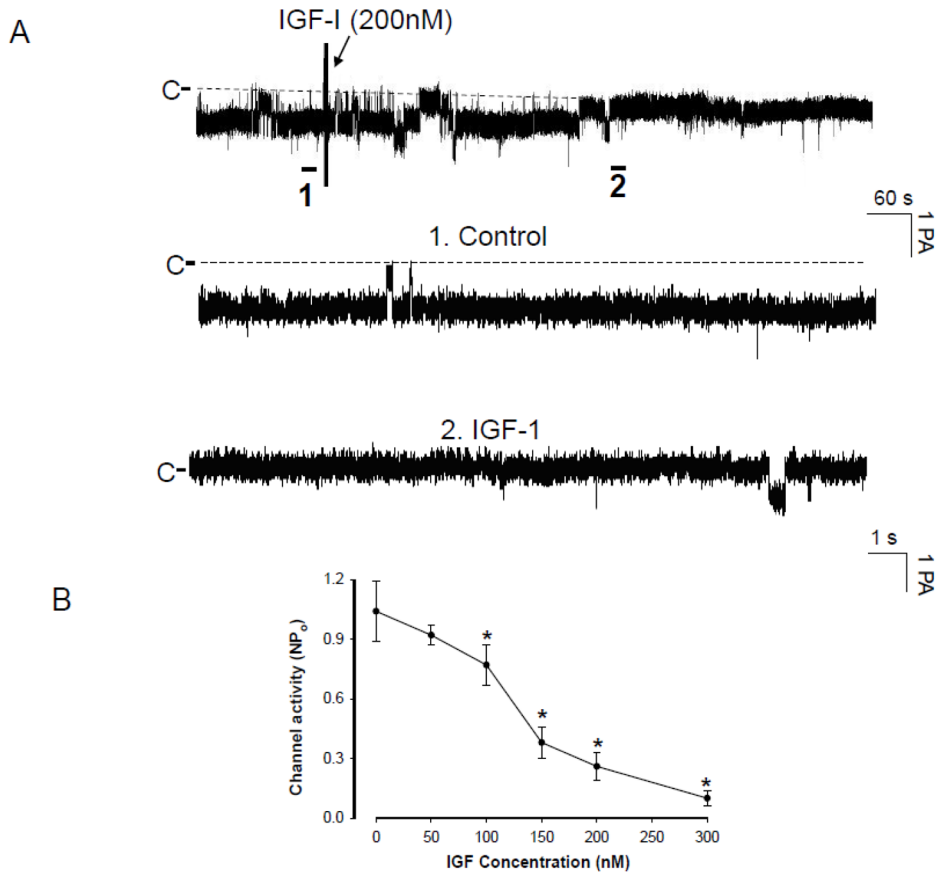

Fig. 1.

(A) A channel recording demonstrating the effect of IGF-1 on the 10-pS Cl channels in the medullary TAL. The experiments were performed in cell-attached patches and the holding potential was -60 mV. The arrow indicates the addition of IGF-1. Two parts of the traces indicated by numbers are extended to show the fast time resolution. The channel closed level is indicated by “C” and a dotted line. (B) A dose–response curve of IGF-1’s effect on the Cl channels in cell-attached patches. Asterisk indicates that the difference is significant in comparison to the control value.

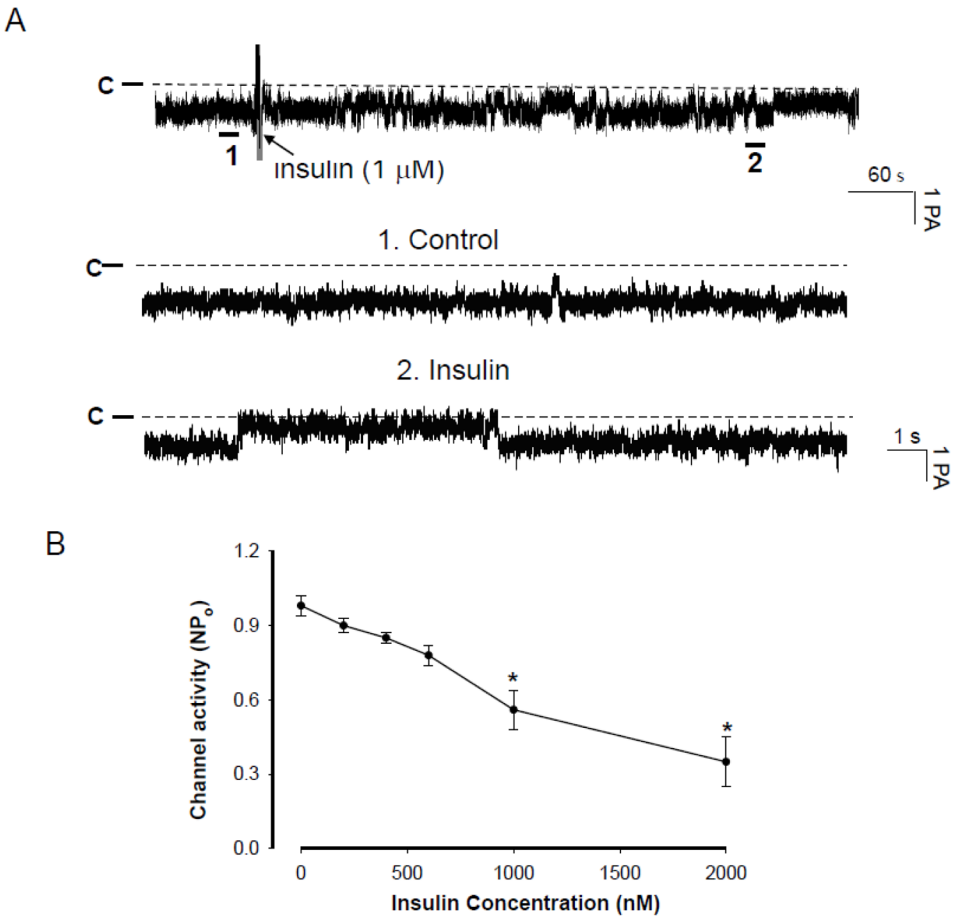

Fig. 2.

(A) A channel recording demonstrating the effect of insulin (1 μM) on the 10-pS Cl channels in the medullary TAL. The experiments were performed in cell-attached patches and the holding potential was −60 mV. The arrow indicates the addition of insulin. Two parts of the traces indicated by numbers are extended to show the fast time resolution. The channel closed level is indicated by “C” or a dotted line. (B) A dose–response curve of insulin’s effect on the Cl channels in cell-attached patches. Asterisk indicates that the difference is significant in comparison to the control value.

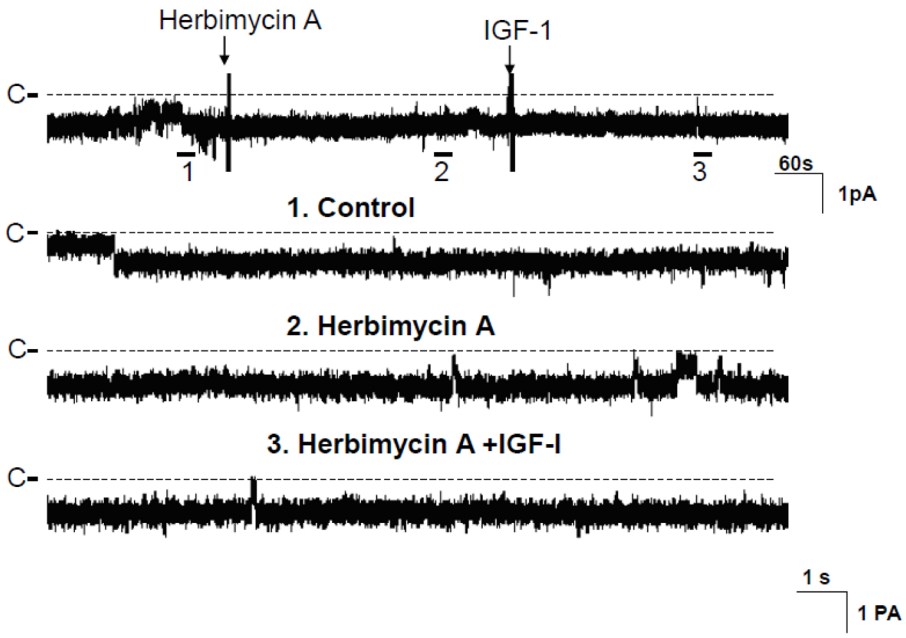

Fig. 3.

A channel recording showing the effect of IGF-1 (200 nM) on the Cl channels in the presence of herbimycin A (1 μM). The top trace shows the time course of the experiments and three parts of the recording indicated by numbers are extended to demonstrate the fast time course. The channel closed level is indicated by "C" and a dotted line. The experiments were performed in cell-attached patch and the holding potential was −60 mV.

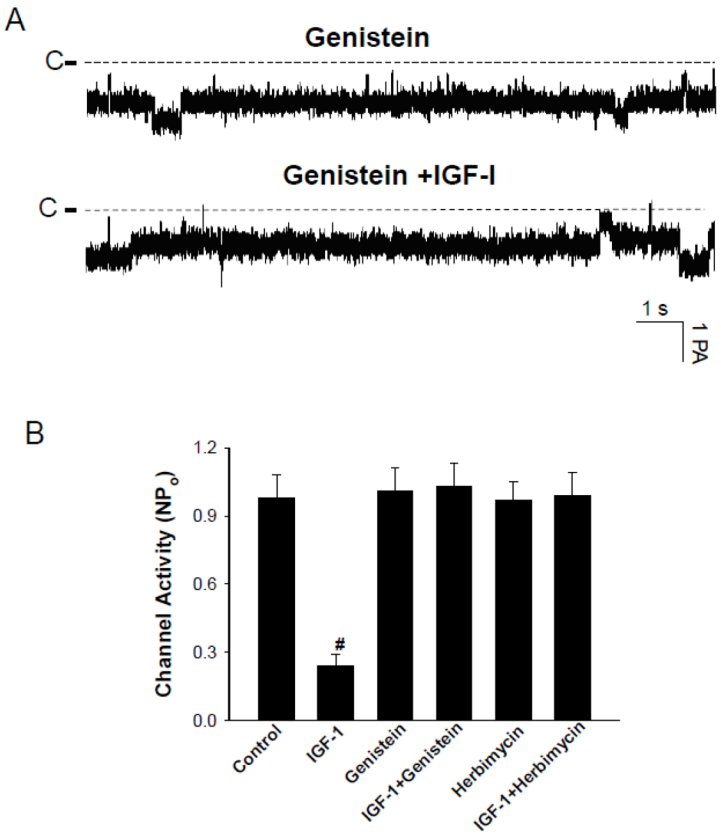

Fig. 4.

(A) A channel recording demonstrating the effect of IGF-1 (200 nM) on the Cl channels in the presence of genistein (10 μM). The channel closed level is indicated by a dotted line and C. The holding potential was −60 mV (hyperpolarization). (B) The bar graph summarizes the results of experiments in which the effect of IGF-1 on Cl channels was examined in the absence or in the presence of Herbimycin A or genistein (control NP_o, 0.98±0.1; IGF-1, 0.24±0.05; genistein, 1.01±0.1; IGF+genistein, 1.03±0.1; Herbimycin A, 0.97±0.08; IGF +Herbimycin A, 0.99±0.1) (n=5–6). "#" indicates a significant difference in comparison to the control.

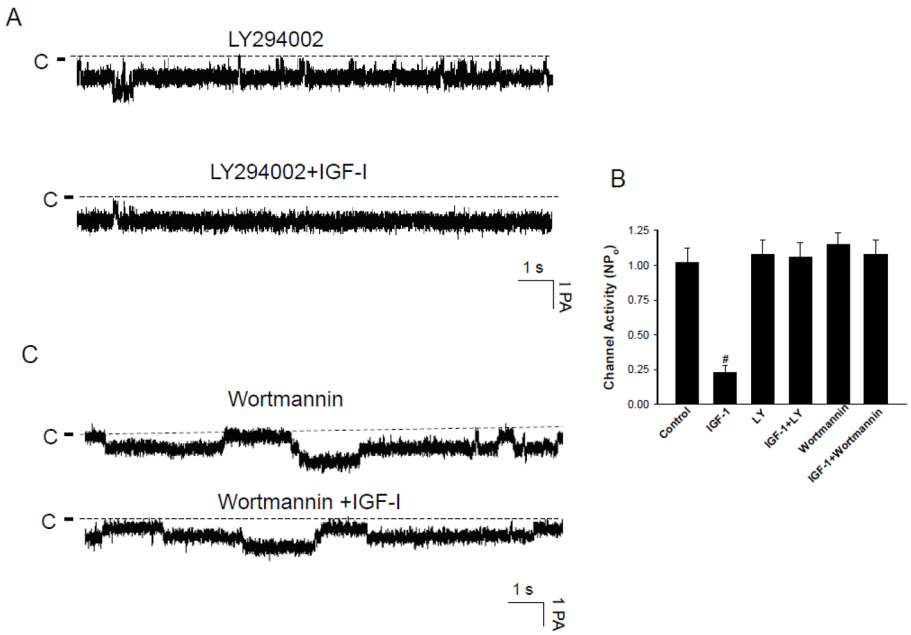

Fig. 5.

(A) A channel recording demonstrating the effect of IGF-1 (200 nM) on the Cl channels in the presence of LY294002 (10 μM). (B) The bar graph summarizes the results of experiments in which the effect of IGF-1 on Cl channels was examined in the absence or in the presence of LY294002 or Wortmannin (control NP_o, 1.02±0.1; IGF-1, 0.23±0.05, Ly294002(LY), 1.08±0.1; IGF+LY, 1.06±0.1; Wortmannin, 1.15±0.08; IGF+Wortmannin, 1.08±0.1) (n=5–7). "#" indicates a significant difference in comparison to the control. (C) A channel recording demonstrating the effect of IGF-1 (200 nM) on the Cl channels in the presence of wortmannin (100 nM). The experiments were performed in cell-attached patch and the holding potential was −60 mV.

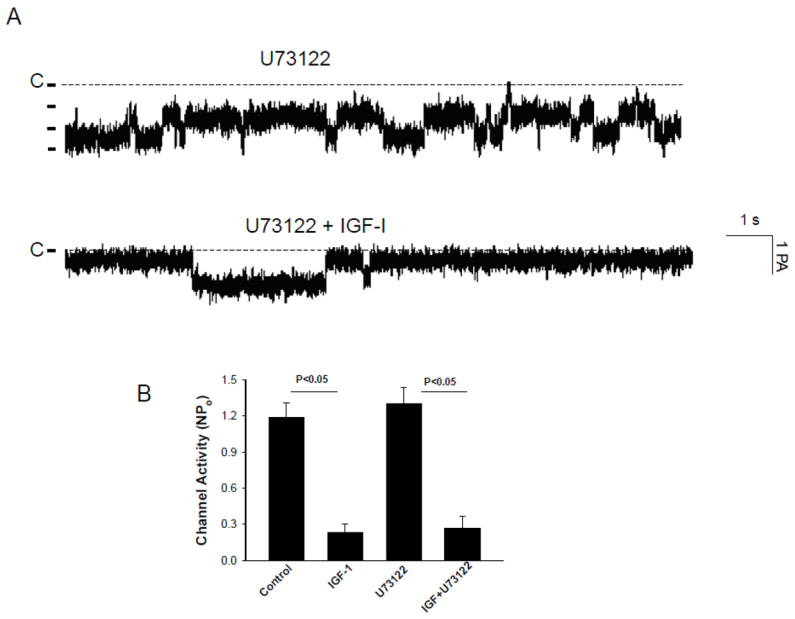

Fig. 6.

(A) A channel recording demonstrating the effect of IGF-1 (200 nM) on the Cl channels in the presence of U73122 (5 μM). (B) A bar graph summarizing experiments in which the effect of IGF-1 on the Cl channels was examined in the presence of U73122 ((control NP_o, 1.19±0.1; IGF-1, 0.23±0.07; U73122, 1.3±0.14; IGF+U73122, 0.27±0.1) (n=4–5) The experiments were performed in cell-attached patch and the holding potential was −60 mV.

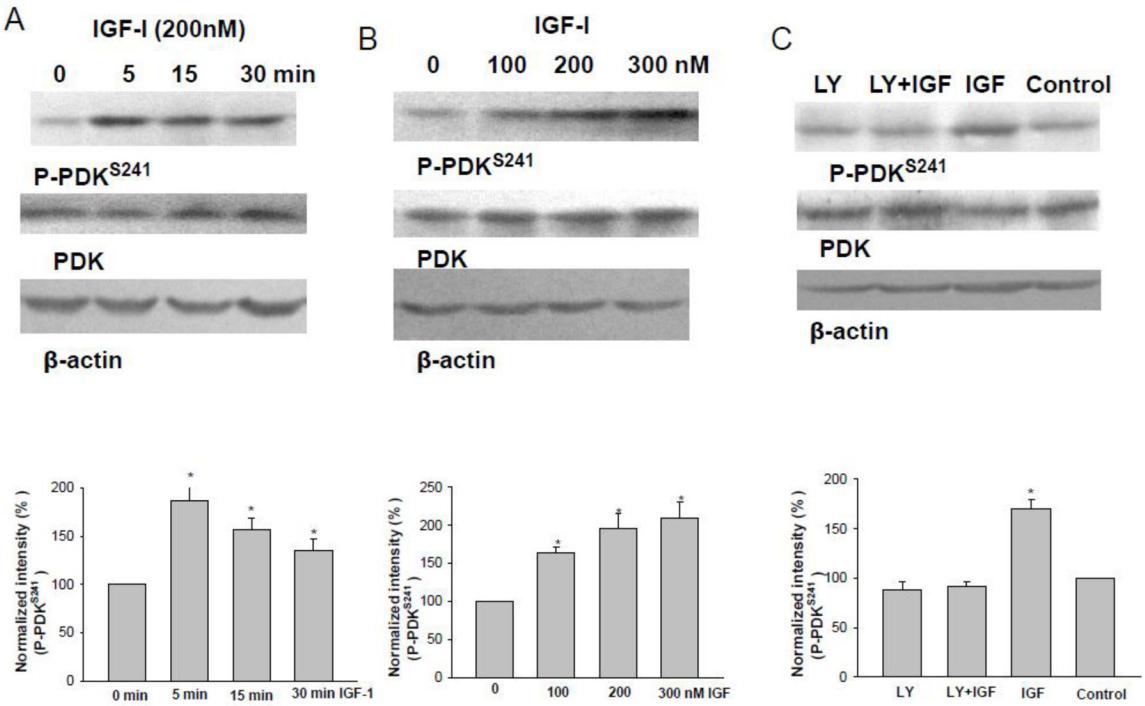

Fig. 7.

(A) A Western blot showing the effect of IGF-1 (200 nM) on PDK phosphorylation with P-PDK^{S241} at 5, 15 and 30 min, respectively. Results were summarized in the bottom of the figure. (B) A Western blot showing the effect of IGF-1 treatment (5 min) on PDK phosphorylation with P-PDK^{S241} at 100, 200 and 300 nM, respectively. Results were summarized in the bottom of the figure. (C) A Western blot showing the effect of IGF-1 treatment (200 nM for 5 min) on the PDK phosphorylation in the medullary TAL treated with or without LY294002. Results were summarized in the bottom of the figure. Asterisk indicates a significant difference in comparison to the control.

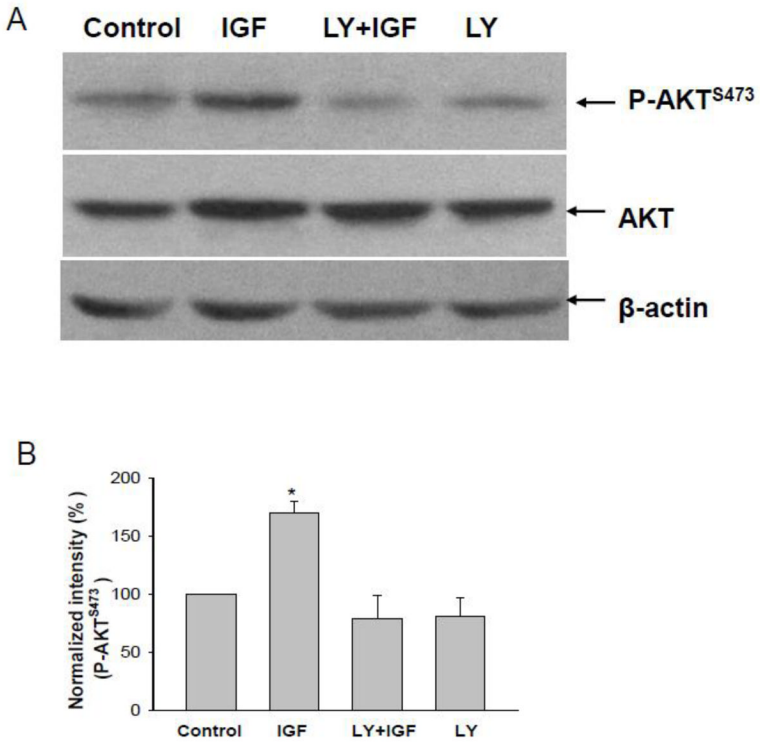

Fig. 8.

(A) A Western blot showing the effect of IGF-1 treatment (200 nM for 5 min) on the AKT phosphorylation in the medullary TAL treated with or without LY294002 (10 μM). (B)Results were summarized in the bottom of the figure. Asterisk indicates a significant difference in comparison to the control.

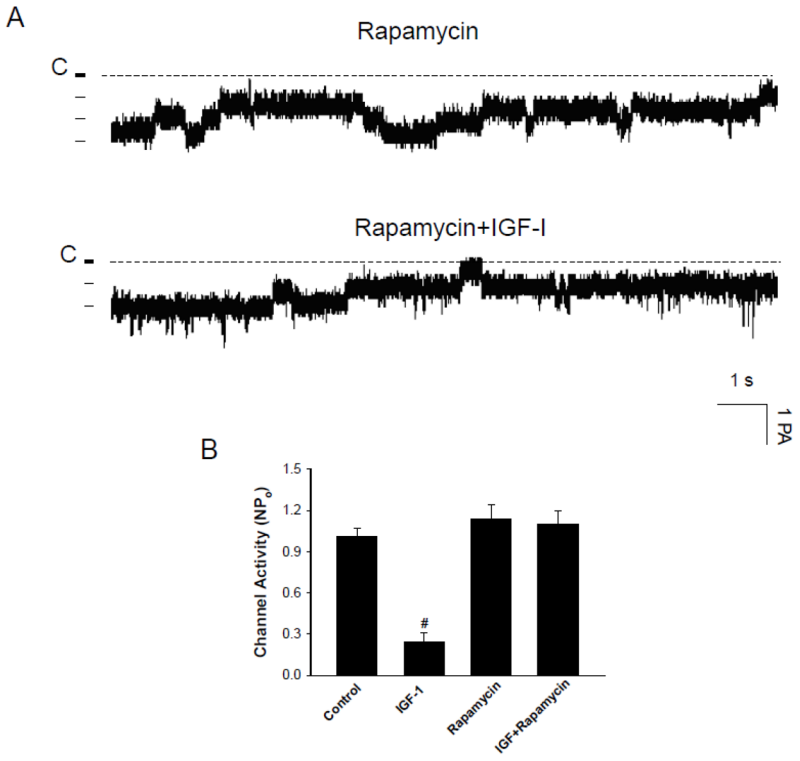

Fig. 9.

(A) A channel recording demonstrates the effect of 200 nM IGF-1 on the 10-pS Cl channels in the presence of rapamycin (100 nM). The experiments were performed in cell-attached patches and the holding potential was −60 mV. (B) A bar graph summarizing experiments in which the effect of IGF-1 on the Cl channels was examined in the presence of rapamycin (control NP_o, 1.01±0.1; IGF-1, 0.24±0.06;; rapamycin, 1.14±0.1; IGF+rapamycin, 1.1±0.1) (n=4–5). “#” indicates a significant difference in comparison to the control.

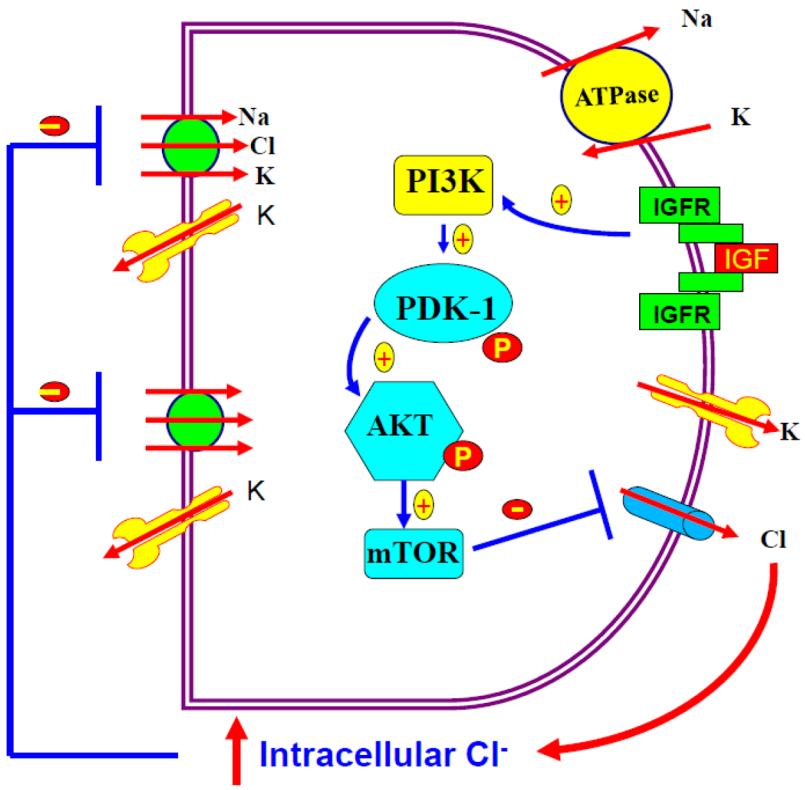

Fig. 10.
A cell model illustrating the role of IGF-1 at high concentrations in inhibiting transepithelial Cl